

## Interparticle coupling effects in nanofabricated substrates for surface-enhanced Raman scattering

L. Gunnarsson, E. J. Bjerneld, H. Xu, S. Petronis, B. Kasemo, and M. Käll<sup>a)</sup>

*Department of Applied Physics, Chalmers University of Technology, S-41296 Göteborg, Sweden*

(Received 22 June 2000; accepted for publication 28 November 2000)

Surface-enhanced Raman scattering (SERS) substrates, consisting of arrays of electromagnetically coupled Ag nanoparticles on Si, were manufactured by electron-beam lithography. Substrate Raman efficiency, evaluated from the relative SERS intensities of the adsorbates rhodamine 6G and thiophenol, was found to increase rapidly with decreasing interparticle separation, signaling the importance of strong interparticle coupling effects in SERS. The observed SERS efficiency variation can be qualitatively explained in terms of electrostatic models of coupled metal structures. © 2001 American Institute of Physics. [DOI: 10.1063/1.1344225]

The surface-enhanced Raman scattering (SERS) technique has gained a reputation as one of the most sensitive spectroscopic tools available for the detection of a wide range of adsorbate molecules down to the single molecule detection limit.<sup>1–4</sup> The SERS effect is predominantly of electromagnetic origin, i.e., due to an increase in the local optical field exciting the molecule and a multiplicative amplification of the re-radiated Raman scattered light.<sup>1</sup> This requires that the molecule is situated in the vicinity of a mesoscopically structured metal surface, preferably one that supports an electromagnetic resonance at the excitation and/or emission wavelength involved in the Raman scattering process. Since the pioneering work of Liao *et al.*<sup>5</sup> several lithographic techniques have been employed for the production of more uniform and controllable SERS substrates<sup>6–9</sup> than is possible to achieve in traditional systems based on, e.g., “roughened” Ag or Au surfaces, metal island films, or colloidal suspensions.<sup>1</sup> One of the most interesting possibilities with the lithographic approach is to achieve a controlled electromagnetic coupling between metal particles, an effect which is known to give a dominant contribution to the SERS efficiency of aggregated colloidal systems.<sup>1,2,4</sup> In this letter we demonstrate that large interparticle coupling effects can be generated in SERS substrates fabricated with electron-beam lithography. This finding opens up a range of interesting possibilities for applications based on optically active nanofabricated structures, including, e.g., SERS sensors integrated in “lab-on-a-chip” type systems, substrates for nonlinear optical spectroscopies or structures optimized for photoassisted catalysis.

The present SERS substrates consists of arrays of Ag particles on SiO<sub>2</sub>/Si. A single or double-layer resist was spin coated on a clean Si wafer, with (100) surface covered by native oxide, and the pattern was defined by electron-beam lithography. Removal of the exposed resist with a developer was followed by vapor deposition of a 30–40 nm thin Ag layer, after which the unexposed resist was dissolved (see Ref. 9 for further details of the manufacturing process). The latter step removes the unwanted Ag areas through the liftoff

process. The structures were examined in a scanning electron microscope before and after SERS measurements. The arrays were defined by the particle length-scale  $D$ , interparticle separation distance  $d$ , and particle shape (triangular, square, or circular); Fig. 1 shows SEM images of typical structures. Two different probe molecules, rhodamine 6G (R6G) and thiophenol, were used for evaluation of the samples SERS efficiencies. The adsorbates were applied through incubation of the cleaned SERS substrates in either 10 nM R6G in water or 10 mM thiophenol in ethanol. Raman backscattering measurements were performed in a microscope setup (100×, NA = 0.95) with the incident 514.5 nm laser-light polarized along the main symmetry axis of the arrays. The scattered light was passed through a holographic notch filter, resolved by a single-grating spectrometer and detected with a LN<sub>2</sub>-cooled charge-coupled-device (CCD) camera. The probe area was 1–2 μm in diameter and the incident power ranged between 0.2 and 1 mW. Accurate relative SERS efficiencies were achieved through calibration against the 520

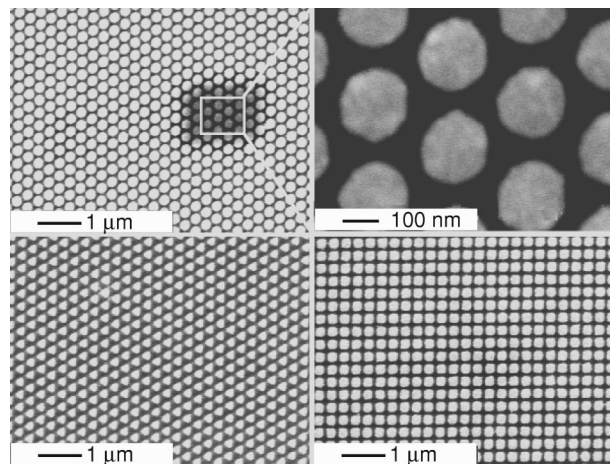


FIG. 1. Scanning electron micrographs of SERS substrates. Examples consists of circular (top left and right), triangular (bottom left), and square (bottom right) 30-nm-thin Ag particles on Si. The predefined particle length scale, defined as the diameter in the case of circular particles and the edge length in the case of triangles or squares, was  $D=200$  nm and the predefined interparticle separation distance, defined as the minimum edge-to-edge distance, was  $d=100$  nm.

<sup>a)</sup>Electronic mail: kall@fy.chalmers.se

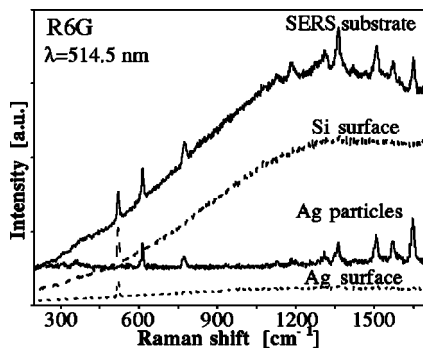


FIG. 2. Illustration of SERS-substrate efficiency. Samples were incubated with 1 nM rhodamine 6G and investigated successively without changing the experimental parameters. Spectra from top to bottom are: nanofabricated SERS substrate (circular particles,  $D=100$  nm,  $d=50$  nm); flat Si surface; dense layer of Ag nanoparticles; and unstructured flat Ag surface on Si. Note the intense Si line at  $520\text{ cm}^{-1}$  used as an internal intensity calibration standard. The Ag nanoparticles were of the same type as used for single-molecule SERS of hemoglobin, as reported in Ref. 4.

$\text{cm}^{-1}$  Si phonon (intensity proportional to area not covered by Ag).

Figure 2 shows a collection of spectra that illustrates the efficiency of the nanofabricated SERS substrates. R6G adsorbed directly on Si exhibits an intense fluorescence<sup>10</sup> but no visible R6G Raman bands; R6G adsorbed on an unstructured flat Ag layer deposited on Si exhibits a more-or-less quenched fluorescence but still no Raman features, while R6G adsorbed on a nanostructured SERS substrate produces R6G Raman features comparable in strength to what is obtained for R6G adsorbed on a layer of highly SERS-active Ag nanocrystallites.

In order to investigate the variation in SERS intensity with varying particle characteristics, a range of  $100\ \mu\text{m}^2$  particle arrays were prepared on the same Si wafer and examined in succession. Figure 3 demonstrates that a decrease in the interparticle separation distance  $d$  results in a clear increase in the recorded SERS intensity for both probe molecules. The effect is most dramatic for the thiophenol data, which exhibits a fifty-fold signal increase when going from the longest ( $d\approx 250$  nm) to the shortest ( $d=75$  nm) separation distances. A decrease in the particle size  $D$  leads to a comparatively weak increase in efficiency, an effect most pronounced for samples with small  $d$  values, while the particle shape seemed to have little or no influence on the overall substrate performance.

The data in Fig. 3 can be qualitatively explained with the following simple model. Assume that the measured SERS signal consists of two contributions:

$$I^{\text{SERS}} \propto N^{\text{edge}} M^{\text{edge}} + N^{\text{top}} M^{\text{top}} \quad (1)$$

where  $N^{\text{top}}$  and  $N^{\text{edge}}$  are the number of adsorbed molecules at the upper surfaces and at the edges of the Ag particles, respectively, and  $M^{\text{top}}$  and  $M^{\text{edge}}$  are the corresponding SERS enhancement factors. For a given measurement area and particle thickness, the number of adsorbed molecules will scale as  $N^{\text{edge}} \propto D/(D+d)^2$  and  $N^{\text{top}} \propto D^2/(D+d)^2$ . As an approximation, sufficient for the present purpose, we consider the enhancement factors as composed of two parts—a single-particle contribution, independent of  $d$ , and a contribution due to interparticle coupling, varying with  $d$ . The lat-

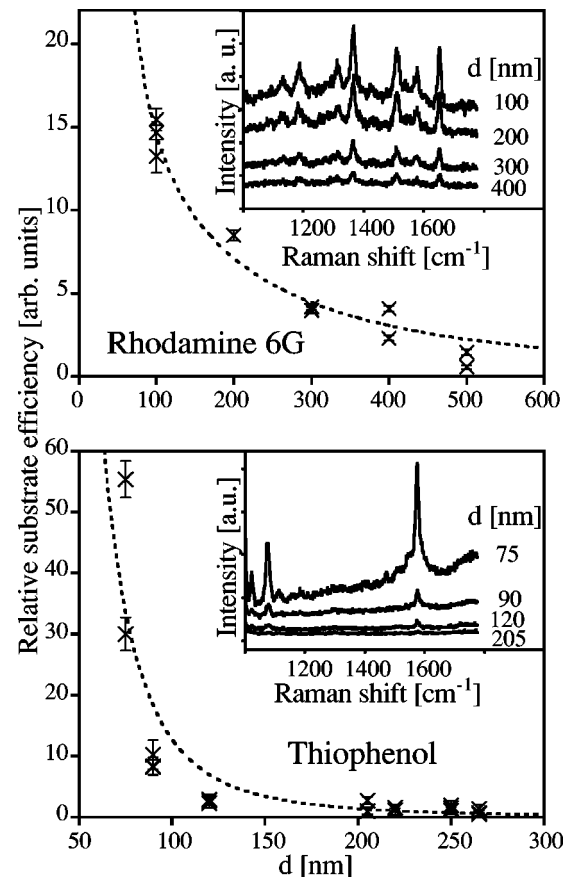


FIG. 3. Relative SERS-substrate efficiency vs  $d$ , quantified as  $I^{\text{SERS}}(d)/I^{\text{SERS}}(d^{\text{max}})$ , for two different adsorbates: R6G (circular particles,  $D=200$  nm) and thiophenol (square particles,  $D=200$  nm). Insets show examples of Raman spectra for different  $d$  values. Dashed lines are fits using the electrostatic model  $I^{\text{SERS}} \propto (d+D)^{-2}[A(D/d+1)^4+B]$ , where  $A$  and  $B$  are fitting constants.

ter can be visualized as follows: Imagine a row of particles of length  $D$  separated by gaps of length  $d$  arranged parallel to a uniform electrostatic field  $E_0$ . If the particles are perfectly conducting, the electrostatic potential drop will be concentrated to the interparticle region, resulting in a local field  $E_L = E_0(D+d)/d$ . A molecule placed in the interparticle region thus experiences an exciting intensity that is enhanced by a factor  $(D/d+1)^2$  over the free-space value. The same enhancement will also affect the Raman scattered field, provided this is aligned parallel to the particle row, resulting in a net enhancement of the order  $(D/d+1)^4$ . We assume that  $M^{\text{edge}}$  is dominated by this interparticle enhancement, while  $M^{\text{top}}$  is dominated by the single particle enhancement, i.e.,  $M^{\text{top}} \approx \text{constant}$ . Combining the results above yields a function appropriate for data-analysis:

$$I^{\text{SERS}} \propto (d+D)^{-2}[A(D/d+1)^4+B], \quad (2)$$

where  $A$  and  $B$  are fitting constants.

The curve fits in Fig. 3 show that the simple model above adequately describes both sets of  $d$  dependent data. Note in particular that Eq. (2), with  $B=0$ , accurately predicts the rapid increase in substrate efficiency for thiophenol, setting on around  $d=100$  nm, in this case demonstrating a *dominant interparticle coupling contribution* to the overall surface enhancement. The considerably weaker  $d$  dependence for R6G, with  $A(D/d+1)^4/B \approx 0.1$  at  $d=100$  nm,

probably originates from the different adsorption characteristics of R6G compared to thiophenol. Whereas the latter exhibits a specific binding to Ag, i.e., chemisorption via the thiol group with the phenol ring pointing out from the surface, the R6G molecule can be expected to be oriented with its large and easily polarizable ring structure laying flat on the surface. If this is the case, the Raman scattered light will be polarized parallel to the surface. This means that the interparticle coupling contribution, which requires a polarization perpendicular to the particle-edge surface, will decrease while the contribution from molecules at the upper particle surfaces will increase.

In conclusion, we have fabricated substrates for surface-enhanced Raman scattering that exhibits a controlled electromagnetic coupling between Ag nanoparticles. Our results suggest that state-of-the-art nanofabrication is a powerful route towards optimized SERS substrates and other applications that require a control of optical processes at mesoscopic length scales.

One of the authors (M.K.) gratefully acknowledges financial support from the Swedish Foundation for Strategic Research and stimulating discussions with Peter Apell on the

theoretical modeling. L.G. is supported by the Swedish Research Council for Engineering Sciences.

- <sup>1</sup>For a review see, M. Moskovits, *Rev. Mod. Phys.* **57**, 783 (1985).
- <sup>2</sup>K. Kneipp, Y. Wang, H. Kneipp, L. T. Perelman, I. Itzkan, R. R. Dasari, and M. S. Feld, *Phys. Rev. Lett.* **78**, 1667 (1997).
- <sup>3</sup>S. Nie and S. R. Emory, *Science* **275**, 1102 (1997).
- <sup>4</sup>H. Xu, E. J. Bjerneld, M. Käll, and L. Börjesson, *Phys. Rev. Lett.* **83**, 4357 (1999).
- <sup>5</sup>P. F. Liao, J. G. Bergman, D. S. Chemla, A. Wokaun, J. Melngailis, A. M. Hawryluk, and N. P. Economou, *Chem. Phys. Lett.* **82**, 355 (1981).
- <sup>6</sup>R. L. Moody, T. Vo-Dinh, and W. H. Fletcher, *Appl. Spectrosc.* **41**, 966 (1987).
- <sup>7</sup>J. C. Hulteen, D. A. Treichel, M. T. Smith, M. L. Duval, T. R. Jensen, and R. D. Van Duyne, *J. Phys. Chem. B* **103**, 3854 (1999), and references therein.
- <sup>8</sup>M. Kahl, E. Voges, S. Kostrewa, C. Vietz, and W. Hill, *Sens. Actuators B* **51**, 285 (1998).
- <sup>9</sup>L. Gunnarsson, S. Petronis, B. Kasemo, H. Xu, J. Bjerneld, and M. Käll, *Nanostruct. Mater.* **12**, 783 (1999).
- <sup>10</sup>The fluorescence signal from the type of structures produced here can be expected to depend on the balance between two competing phenomena: fluorescence quenching, experienced by molecules adsorbed to the Ag particles, and fluorescence enhancement, due to an increase in the local fields experienced by molecules adsorbed to exposed Si in the interparticle regions.